CRITICAL CONDITIONS FOR MICRODAMAGE INITIATION IN A SPALLING METAL

V. K. Golubev, S. A. Novikov,
Yu. S. Sobolev, and N. A. Yukina

UDC 539.4

An experimental study [1] has been made on the effects of temperature on the critical loading conditions corresponding to macroscopic spalling damage for various metals, where the object was to determine the maximum mechanical strength of the metal with a characteristic loading time of about 1 μsec. Nevertheless, numerous papers such as [2] indicate that the spalling microdamage occurs at much lower loading levels. The critical loading conditions corresponding to spalling microdamage are of considerable scientific and practical interest, since the avalanche production of a large amount of microdamage characterizes the exhaustion of the physical strength, while the damage levels themselves are related to the complicated dislocation kinetics in the accumulation of damage at the submicroscopic level.

We have used the metals examined in [1] to determine the critical loading conditions corresponding to spalling microdamage at a normal test temperature (about 0°C). Detailed metallographic analysis has been used to determine the character of the damage, while measurements were also made of the microhardness in the initial and loaded states in order to provide a more rigorous comparison with other tests.

The results from the experiments have been partly given in [1], where critical loading levels were determined that correspond to macroscopic spalling failure. The scheme used in the experiments was also given there, together with the dimensions of the specimens and the method of evaluating the pulsed mechanical loading conditions. We tested specimens from the same batches as in [1], and also some new specimens made of Armco iron of thickness 20 mm. Pulsed mechanical loading was provided by impact of an aluminum plate of thickness 4 mm. After loading, each specimen was sectioned and the surface of the section was polished and etched and was observed under the microscope at a magnification of up to 1000. This enabled us to compare the known rate of collision with the degree of spalling damage and also to determine the critical loading conditions for spalling microdamage.

Estimates of the pressure in the loading pulses were made on the basis of the shock adiabatics for the materials [1]. The characteristic loading time was 1.3-1.5 μsec, where the limits correspond to the circulation times for the elastic and plastic waves in the aluminum striker. Several experiments were also performed to measure the pulse pressures in the materials with a manganin transducer with the apparatus of [3]. Figure 1 shows the waveform from one of the experiments with AMg6 aluminum alloy. In the experiment, two transducers were in the same plane at a distance of 5 mm from the loaded surface, while the distance between them was 50 mm. The frequency of the time markers was 1 MHz, while the pressure was calibrated at 0.95 GPa. The measured pressure amplitude exceeded the value estimated from the shock adiabatic, but within the accuracy of the method (10%) it agreed with the estimate from the elastoplastic model. As the impact velocity increased, there was a reduction in the discrepancy between the experimental results and the estimates made from the shock adiabatic. The characteristic time at half-height in the pulse was close to 1.5 μsec, while the time spread in the collision as estimated from the displacement of the amplitude values was 0.5 μsec, which corresponds to a tilt angle on collision of about 25''.

Figure 2 shows the results, where the loading-pressure level is compared with the fall in damage as determined by metallographic examination of longitudinal sections. The following gradations are used for the damage: 1) complete spalling damage, with the principal spalling crack passing through the entire cross section; 2) partial macroscopic damage, namely individual macroscopic cracks in the section; 3) extensive microscopic damage, with isolated or fusing microcracks or pores considerable in numbers in the spalling zone; 4) slight microscopic damage, with a few isolated areas of damage in the spalling zone or some

Moscow. Translated from Zhurnal Prikladnoi Mekhaniki i Tekhnicheskoi Fiziki, No. 4, pp. 151-158, July-August, 1983. Original article submitted July 7, 1982.

 0021-8944/83/2404-0586$07.50

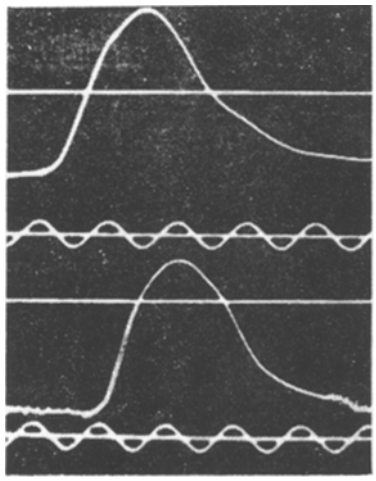

Fig. 1

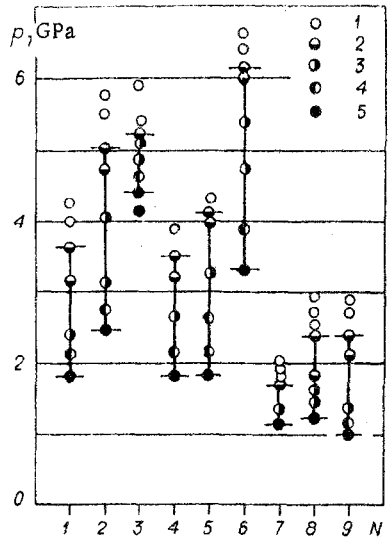

Fig. 2

parts of it; and 5) retention of microscopic integrity, with the absence of microscopic damage observable at ×1000 magnification. This numbering is used also in Fig. 2. The limiting values for the ranges in Fig. 2 correspond to the critical loading conditions representing spalling microdamage and also complete macroscopic failure. Figure 2 also gives the numbers of the materials along the abscissa in the following sequence: 1) M1 copper, 2) NP2 nickel, 3) VT14 titanium alloy, 4) Armco iron, 5) St. 3 steel, 6) 12Kh18N10T steel, 7) AD1 aluminum, 8) D16 aluminum alloy, and 9) AMg6 aluminum alloy.

As regards the tensile stress in the spalling zone, this was p_* in the acoustic approximation, where p_* is the critical value of the pressure in the loading pulse corresponding to spalling microdamage. If the loading pressure exceeds p_*, the tensile stress in the spalling zone evidently remains at about the same level corresponding to p_*. This has been observed for example in [4] and is ascribed to stress relaxation at the damage formed and growing during the loading.

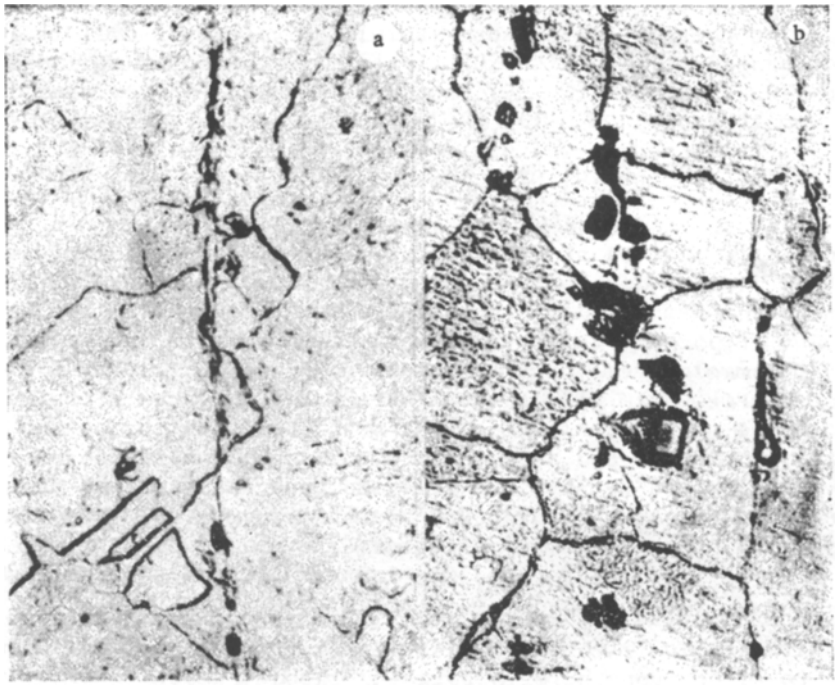

Fig. 3

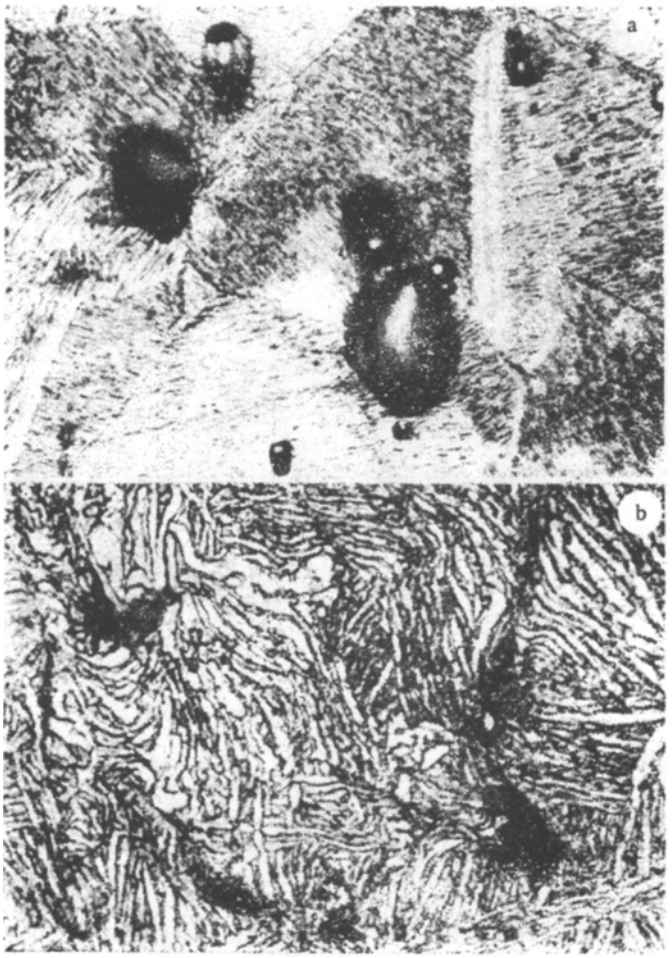

Fig. 4

Detailed metallographic analysis was performed for all the specimens. This indicated the extent of damage at various loading levels, the character of the damage initiation and development at the structural level, and also some of the most prominent changes in the structure due to the specific loading conditions. Figures 3-6 show some of the metallographic results at a magnification of ×800. We briefly describe the spalling microdamage.

In copper, the characteristic damage is formed mainly as small zones of extensive local plastic deformation elongated in the rolling direction (Fig. 3a), and the damage to and expansion of these lead to elongated bands. There are also small pores, but their contribution to the damage is slight. In nickel, one finds a similar type of damage, although the local deformation and damage zones as a rule are shorter and wider. However, this type of damage is not dominant here. A rough visual evaluation indicates that the damage due to the initiation and growth of pores (Fig. 4a) contributes about half of the damage in the nickel. In 12Kh18N10T steel, damage in the form of pores occurs at clumps of inclusions elongated in the rolling direction (Fig. 3b) [5]. In VT14 titanium alloy, the initiation occurs as fairly viscous microcracks (Fig. 4b) formed mainly at the grain boundaries. Individual cavities are also formed at points where the cracks meet. In Armco iron, the microdamage takes the form of cleavage microcracks (Fig. 5a). The damage in steel St. 3 is similar (Fig. 5b) [5]. In AD1 aluminum, the damage takes the form of cavities and viscous microcracks (Fig. 6a). There is a minor contribution to the overall damage from the small pores (Fig. 6b). In D16 and AMg6 aluminum alloys, the damage takes the form of cavities of irregular shape occurring at clumps of inclusions (Fig. 6c and d).

There are certain structure changes in these metals that can be observed by metallography. For example, in Armco iron there is twinning in the ferrite grains in the impact zone at a depth up to 6 mm, which has been observed previously [5] for steel St. 3. In [5] it was also observed that austenite is transformed to martensite at 0°C in the spalling zone in

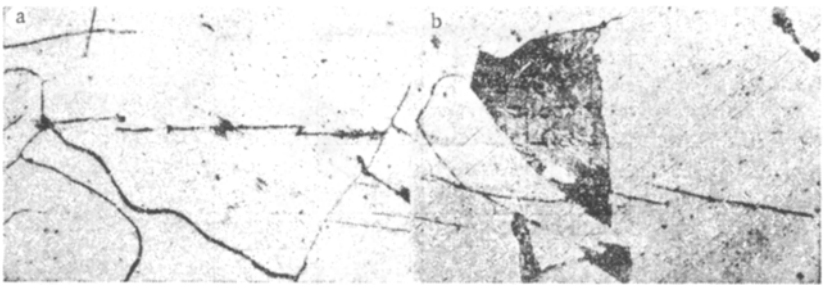

Fig. 5

12Kh18N10T steel. More careful metallographic examination showed that a less pronounced martensite transformation occurs also in the impact zone at a depth up to 6 mm. This was confirmed also by microhardness measurements, which are dealt with separately.

The measurements on the microhardness H_μ were made in the initial state and after loading. As the specimens were made as rods in the state as supplied and were not annealed, there was no substantial change in H_μ. The only exception was represented by 12Kh18N10T steel, where there was a change in microhardness due to the formation of martensite. The value of H_μ measured at a load of 100 g was 1.96 GPa for this steel in the initial state, while for a specimen tested for example at 6 GPa there was a gradual decrease in the microhardness from 2.84 to 2.34 GPa as the distance from the loaded surface increased up to 6 mm. Nevertheless, there was more complete transformation in the spalling zone, which was responsible for extensive local plastic deformation, and here H_μ was 3.15 GPa. In St. 3 steel, the value of H_μ for the ferrite was 1.80 ±0.04 GPa (standard deviation), while for pearlite it was 3.43 ±0.24 GPa. The values for iron, VT14 alloy, nickel, and copper were H_μ = 1.48 ± 0.05; 3.79± 0.11; 2.11± 0.08 and 0.83 ±0.02 GPa, and for copper there was a slight rise in the microhardness in the impact zone. For example, for the specimen tested at 2.4 GPa there was a gradual reduction in the microhardness with distance from the loaded surface up to 7 mm, namely from 0.92 to 0.85 GPa. Also, in each case we measured not less than 20 indents, with the load 200 g for VT14 alloy or 50 g for the other materials.

These results may be compared with others. Figure 7 gives some of the existing results on the effects of loading time τ on p_*. Figure 7a gives results for aluminum and its alloys D16 (2024) and AMg6: 1) our results, mean values for aluminum and the alloys, 2) aluminum, annealing, characteristic damage as viscous pores [2], 3) 2024 alloy, characteristic damage viscous cracks [2], 4) 1145 aluminum, preliminary annealing, viscous pores [2], 5 and 6) AMg6 alloy, specimens made from rod and sheet [6], 7) 2024 alloy [7]. Figure 7b gives results for copper: 1) our results, 2) cold-rolled copper (99.9%), hardness HRF = 68 [8], 3) OFHC copper, preliminary annealing, pores and cracks [2], 4) OFHC copper of medium hardness, pores and cracks [2]. Figure 7c gives results for iron and low-carbon steel St. 3: 1) our results, 2) iron (99.99%) [2], 3) low-carbon steel 1020 [9], and 4) Armco iron [2]; characteristic damage in all cases brittle cracks.

There is a certain spread in the results, but ours agree well with those found previously. This confirms that the results obtained here for VT14 alloy, 12Kh18N10T chromium–nickel steel, and nickel are reliable while being novel. As regards the results for aluminum and copper, the manufacturing technology and subsequent heat treatment affect the strength on short-term loading. Soft plastic metals such as aluminum and copper can show a doubling of the physical strength corresponding to spalling microdamage as a result of preliminary hardening during rolling, and there is also an increase in the mechanical-strength limit corresponding to macroscopic spalling. As regards the effects of loading time on the microdamage limit, one can only say that there is a clear-cut tendency for the strength to increase as the time decreases, but at present the actual shape of the trend and the physical interpretation are not clear. In principle, the damage during spalling does not differ from that under static conditions of uniaxial stretching [10, 11].

It is of interest to compare the results for Armco iron and low-carbon steel St. 3 with those for aluminum and the D16 and AMg6 alloys. For iron and St. 3, the pressures corresponding to microdamage initiation coincide closely, although it should be noted that on careful metallographic observation two microcracks were observed in the iron specimen. Nevertheless, the strength of the ferrite in the iron and the St. 3 was the same for both under the

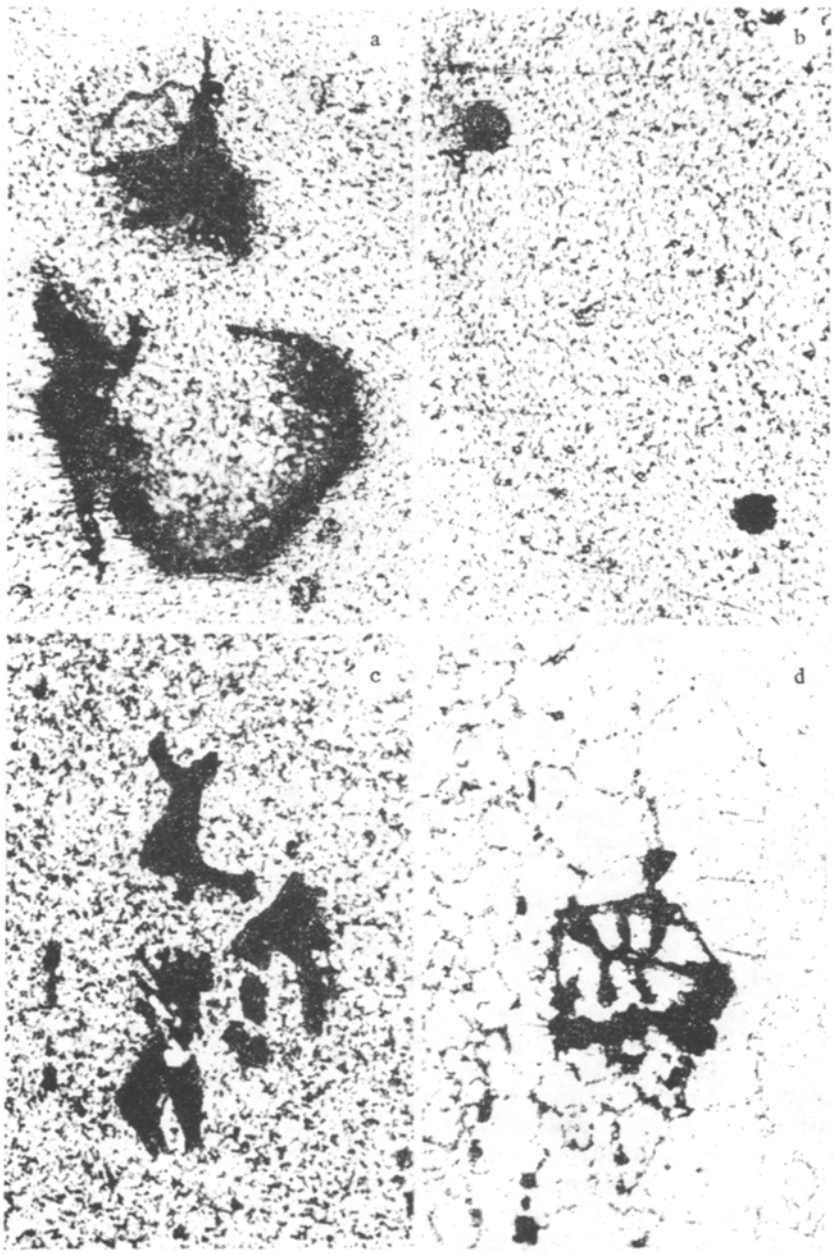

Fig. 6

particular test conditions and within the maximum error of about 10%, while the slight discrepancy was closely correlated with the microhardness measurements. On the other hand, the pressures corresponding to macroscopic damage were substantially different, which was due to the presence of the stronger pearlite in the St. 3, which retards the damage growth in the spalling zone. A somewhat different picture occurs for the aluminum alloys. Here the initial stage of damage is associated with the formation and fusion of damage at clumps of inclusions elongated in the rolling direction, i.e., there is initially longitudinal damage in the spalling zone, while the transverse damage occurs in the later stage, and this is not favored by energy as regards the complete macroscopic failure. This phenomenon occurs to a certain extent in the spalling of other materials made from rods, i.e., having a pronounced longitudinally elongated structure, but it is particularly so when there are many inclusions forming clumps that are elongated in that direction.

The substantial difference in loading levels between the start of microdamage and complete macroscopic failure has been discussed in [12]. There the difference in levels was ascribed to the width of the spalling zone, which also to a considerable extent is related

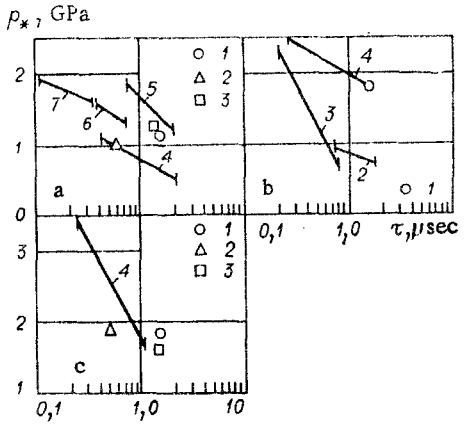

Fig. 7

to the profile of the loading pulse: With a more gently rising front, the damage occurs over a wider zone, which is also disfavored by energy for complete macroscopic damage.

An interesting point is that there is agreement between the results obtained on the critical load levels corresponding to microdamage initiation and those obtained from recording the speed of the free surface during spalling under conditions where the loads exceed the critical levels, sometimes very considerably. The following are for example some values of the critical negative pressures obtained by this method as occurring in the spalling zone on very strong loading. For steel St. 3 and Armco iron [13, 14] 1.7 GPa, for steel 304 (12Kh18N10T) 3.0 GPa [4], and for aluminum 1.2 GPa [15]. This indicates that the negative pressure in the spalling plane under conditions of high-intensity loading does not exceed the level corresponding to the critical level for the initiation of damage in low-intensity loading with similar loading times.

LITERATURE CITED

1. V. K. Golubev, S. A. Novikov, et al., "The effects of temperature on the critical spalling conditions for metals," Zh. Prikl Mekh. Tekh. Fiz., No. 4 (1980).
2. L. Davison and R. A. Graham, "Shock compression of solids," Phys. Rep., 55, No. 4 (1979).
3. Yu. V. Bat'kov and E. D. Vishnevetskii, "Apparatus for measuring pulsed pressures with piezoresistive transducers in the range 0.1-20 GPa," in: Abstracts for the Second All-Union Symposium on Pulsed Pressures [in Russian], Izd. VNIIFTRI, Moscow (1976).
4. S. Cochran and D. Banner, "Spall studies in uranium," J. Appl. Phys., 48, No. 7 (1977).
5. V. K. Golubev, S. A. Novikov, et al., "The spalling-failure mechanisms for St. 3 and 12Kh18N10T steels in the temperature range from 196 to 800°C," Probl. Prochn., No. 5 (1981).
6. B. A. Tarasov, "The failure resistance in plates on shock loading," Probl. Prochn., No. 3 (1974).
7. R. M. Schmidt, F. W. Davies, et al., "Temperature dependent spall threshold of four metal alloys," J. Phys. Chem. Solids, 39, No. 4 (1978).
8. J. H. Smith, "The low pressure spall threshold in copper," in: Dynamic Behavior of Materials, ASTM, Philadelphia (1963).
9. A. L. Stevens and F. R. Tuler, "Effect of shock precompression on the dynamic fracture strength of 1020 steel and 6061-T6 aluminum," J. Appl. Phys., 42, No. 13 (1971).
10. M. F. Ashby, C. Gandhi, and D. M. R. Taplin, "Fracture-mechanism maps and their construction for f.c.c. metals and alloys," Acta Metall., 27, No. 3 (1979).
11. R. J. Fields, T. Weerasooriya, and M. F. Ashby, "Fracture mechanisms in pure iron, two austenitic steels, and one ferritic steel," Met. Trans., 11A, No. 2 (1980).
12. D. J. Steinberg and R. W. Sharp, "Interpretation of shock-wave data for beryllium and uranium with an elastic—viscoplastic constitutive model," J. Appl. Phys., 52, No. 8 (1981).
13. S. A. Novikov, I. I. Divnov, and A. G. Ivanov, "A study of the failure in steel, aluminum, and copper on explosive loading," Fiz. Met. Metalloved., 21, No. 4 (1966).

14. G. I. Kanel' and V. V. Shcherban', "Plastic deformation and spalling in armco iron in shock waves," Fiz. Goreniya Vzryva, No. 4 (1980).
15. C. S. Speight, P. F. Taylor, and A. A. Wallace, "Observations of spallation and attenuation effects in aluminium and beryllium from free-surface velocity measurements," in: Metallurgical Effects at High Strain Rates, Plenum Press, New York–London (1973).

INVESTIGATION OF SPALLING FRACTURE UNDER SHOCK DEFORMATION. MODEL OF A DAMAGED MEDIUM

N. Kh. Akhmadeev

UDC 539.42:620.172.254

In connection with the diverse applications of the action of shocks in engineering and science, the question of the strength of the materials being tested under intensive dynamic action conditions is important. At this time the domain of static and quasistatic rupture under tension has been studied sufficiently well. The kinetic (thermofluctuation) theory of the strength of solids (yielding a dependence of the specimen longevity on the magnitude of the tensile stresses σ and on the temperature T), which is valid for fractures occurring in times from 10^{7}-10^{-3} sec [1] has received great acclaim. For fractures with a $\sim 10^{-6}$ sec time scale there is just a system of test facts that is still inadequate for the complete comprehension of processes occurring under dynamic fracture.

1. Dynamic Spalling Fracture

The spalling fracture of plates, finite thickness targets first subjected to shock loading occurring in very brief times ($\sim 10^{-6}$-10^{-7} sec) during head-on interaction of rarefaction waves moving from the plate free surfaces is considered. In collisions of rarefaction waves with intensity 13 GPa and higher, spall in iron and steel specimens is characterized by the formation of very smooth (specular) fracture surfaces [2] with high purity of the spall surfaces, and is the result of the rarefaction wave collisions in which the reverse $\varepsilon \rightarrow \alpha$ phase transformations are realized. As the level of the rupturing stresses is lowered, the purity of the spall surfaces becomes less and under the action of sufficiently high (4-5 GPa) tensile stresses the domains close to the spall surface are characterized by the presence of a large number of microdamage. This is indicated by available test data from a number of experimental papers on the collision of plates [3-6] in which it is made clear for the materials being tested (metals, polymers) that the intensive formation of microdamage (in the form of flat cracks or round pores) occurs in the zone of action of a tensile impulse, resulting in total fracture (rupture) as they accumulate to a certain critical level, in a section of the plate standing off from the external free surface at a distance approximately equal to the length of the impactor. Microdamages are formed in the rupture zone because of the destruction of the solidity in submicroscopic inhomogeneities (solid phases, particles of insoluble impurities, etc.) under the action of the tensile stresses as well as because of the exposure of already existent submicrocavities (gas bubbles, shrinkage cavities, blisters, etc.). At this time there are no direct methods that permit measurement of the stresses or strains (or other parameters) in the fracture domain, and the spall fracture process is determined by the experimentally determined velocity W(t) of the free target surface, by the thickness of the spalling layer δ^* and the structure of the zones close to the spall surface [3-5], hence, mathematical models must be relied upon to analyze the fracture process.

In investigating spall fractures caused by the action of tensile stresses on the order of 6-8 GPa and higher, and characterized by a quite short fracture delay time after the appearance of the tensile stresses, diagramming the instantaneous spall [7] is completely applicable when a mainline crack is formed immediately upon the attainment of a certain critical (rupture) stress σ^*, which divides the specimen into parts at the site where the stress σ first reaches the value σ^*. Attempts to utilize limit criteria based on the critical fracturing stresses σ^* and their various modifications (for example, taking account of the rate

Ufa. Translated from Zhurnal Prikladnoi Mekhaniki i Tekhnicheskoi Fiziki, No. 4, pp. 158-167, July-August, 1983. Original article submitted June 8, 1982.

 0021-8944/83/2404-0592$07.50